We thank the reviewer for the comments which greatly improves our manuscript.

General comments:

The highlight of this paper is a documentation of the sensitivity of NOx emission estimates on the quality of the meteorological fields and the winds in particular. As shown, these issues are especially critical when the resolution of the observations and the models advances to the km scale. This sensitivity is demonstrated in a clear way, and to my opinion is an important aspect to keep in mind for the development of future regional analysis systems. As such, I am still in favour of publishing these results in ACP.

The revised document has a completely new set of figures and new experiments, which provide more insight into the behaviour of the analysis results. This has improved the paper considerably compared to the ACPD version. Despite this, there are still aspects of the paper that can be improved, as documented below.

It would be good to check the English spelling throughout the document, especially for the parts which changed since the previous version of the document.

We checked the English spelling and grammar throughout the manuscript.

Generally the abstract is not well written and not well structured and should be revised. It should clearly state the aim of the study, the tools and simulations, and the conclusions. See my comments below for further details.

Specific comments:

- Abstract: The first 10 lines of the abstract would be better placed in the introduction, and may be largely removed.

- Abstract: "Accurate observation and modelling of these variations require spatial resolution of order 4 km." This fits well with TEMPO, but for me it is unclear what the quoted length scale of 4km is based on. It is not a result of the paper so I suggest to remove it from the abstract.

We removed this statement from the abstract.

- Abstract: The aim of the study can be provided in more detail. In particular the investigation of the sensitivity of emission inversions on the accuracy of the wind analyses.

- Abstract: What is missing is a description of what is done (the OSSE experiments and tools). The ingredients of the OSSE setup should be explained in a few sentences.

- Abstract: "Last but not least our results show that the information of wind uncertainties is not important for NOx emission estimation." This is unclear. First it is claimed that it is essential that the wind RMSE should be below 1 m/s, which seems to contradict the statement that the wind uncertainty is not important !? See also below.

We have revised the abstract to address these comments and state our objectives and conclusions more clearly.

- Introduction: Is well written, clearly states the aim of the study and contains a good set of references. No further comments.

- Sec 2.1, p4, l12: "RADM2 predicts peak NO2 concentrations and the timing that the peak occurs very well when the mechanism is tested against the representative environmental chamber experiments". Is there a reference?

The statement is cited from the reference (Stockwell et al., 1990). In the revision, we decided to remove this sentence.

- p5, l13: "In our next paper we will discuss the potential benefit from assimilations of chemical observations to improve the meteorological fields." I would suggest to remove this line: it is not interesting for the reader to know about future studies.

We removed this line from the manuscript.

- Tables 2 and 3: For people not familiar with DART and WRFDA these tables are difficult to understand, e.g. terms like "cv_options" and "je_factor" is not meaningful. It would be good to explain these options in the text.

We explained the "cv_options" and "je_factor" in the text as below:

"The options in WRFDA settings is summarized in Table 3. The parameter cv_option indicates the background error options in WRFDA. With cv_option = 3, we use the NCEP background error covariance, which is estimated in grid space by what has become known as the NMC method. The statistics are estimated with the differences of 24 and 48-hour GFS forecasts with T170 resolution, valid at the same time for 357 cases, distributed over a period of one year. The parameter je_factor is the ensemble covariance weighting factor. This factor controls the weighting component of ensemble and static covariances."

- Section 2.4: The description of the emission updates is described in a confusing way. First, time-evolving emissions are introduced. Then it is mentioned that "time-static" emissions are the aim of the study. After that, emission scaling factors are introduced, which change after each assimilation, which seems to contradict the "time-static" remark. Please re-write and explain more clearly how emissions are analysed.

We have attempted to clarify the logic.

The NO_x emissions in the inventory are varying hour by hour. With an hourly assimilation frequency, the emission scaling factors are also updated in each hour. In the OSSE setup, the emission error, which is the difference between the truth and the prior emission, is initialized with a constant fraction error. The prior emission is initialized at 70% of the truth at each hour. We modified the text as below:

"The goal of this work is to constrain hourly evolving emissions at the native model resolution. Here we start with a simple case in which the emission error is a constant fraction at all times of day with the prior

emissions set as 70% of the truth and we investigate the ability of assimilation to recover the original emissions."

- p7, l1: "We calculate a layer dependent Box-Air Mass Factor" This statement is a bit confusing as it suggests that a radiative transfer code is run. I understand that lookup tables from Bucsela et al are used. Please formulate more clearly.

We modified the text as below:

"In NO_2 retrieval algorithm, a layer dependent Box-Air Mass Factor (BAMF) represents the sensitivity of the retrieved NO_2 in a specific layer to the true value in the atmosphere."

"Without running a radiative transfer code, the elements of the BAMF vector are computed as a function of solar zenith angle (SZA), viewing zenith angle (VZA), relative azimuth angle (RAA), terrain reflectivity (Rt), terrain pressure (Pt), atmospheric pressure level, (p) and the NO_2 profile (Bucsela et al., 2013)."

- p7, l6: "We assume clear-sky conditions for all observing scenes." Why is this done? This will increase the number of observations artificially.

We agree this artificially increases the number of observations. However, it provides a useful measure of the best possible performance.

- Table 4: The normal distribution N(200%, 100%). What does this mean? Why are there two percentages? This seems to contradict the notation of normal distributions as given in p7, l32, where I would expect the first number to be the nature run value.

Table 4 shows the relative uncertainty σ_{rel} for clean and polluted scenario. We set the relative uncertainty as a random draw from a Gaussian distribution to avoid using a fixed value, which mimics the real case. The notation given in p7, l32 has the absolute observation uncertainty σ instead of the relative uncertainty σ_{rel}. σ is the observation error standard deviation computed as $\sigma = y^{tr} \cdot \sigma_{rel}$. We added this information in Table 4:

"Table 4. Relative observation uncertainty σ_{rel} in synthetic TEMPO NO_2 column for each scenario."

- p10, l9: "succeeds in recovering the true emissions (Figure 5)." I guess you mean Figure 6? The order of the figures should follow the order of the references to the figures in the text (5 <-> 6).

We updated the order of the figures to follow the order of the references to the figures.

- p11, l5-10: The emission update scheme is explained here. The "scaling factor for t-1" seems to be inconsistent with the discussion in section 2.4, which only mentions updates for e_{i+1}. The two texts seem to be inconsistent. Please explain the emission update process more clearly.

We updated the text in section 2.4 as follows:

"A challenge for updating the emissions in the augmented state vector is the absence of an emission forecast model to evolve the emission variables forward in time. The bottom-up inventory to be optimized

provides hourly-resolved emissions for each model grid point. Instead of treating the emission variables of each hour at a specific location as independent parameters, we update the emission scaling factors at each assimilation cycle. In our emission update scheme, the TEMPO NO_2 observations at time i are assimilated to generate a scaling factor for emissions at time i-1. In this way, the model-observation difference in the NO_2 column will correct the emission of an hour ago instead of the current emission. This approach is reasonable because errors in NO_2 concentration result from errors in previous emissions. Considering the short NO_2 lifetime of three hours in summer daytime, emissions from the previous hour have a large contribution to the NO_2 total mass at the current time. For a given model grid point, we define the emissions of truth (e_{i-1}^t), prior (e_{i-1}^{prior}) and posterior (e_{i-1}^{post}) at time $i-1$. Since we start the assimilation with 70% of true emissions, we have $e_m^{prior} = 0.7e_m^t$ for any time m. After assimilating observations at time i, we compute the scaling factor (S_{i-1}) for emissions at time $i-1$ as follows: $S_{i-1} = e_{i-1}^{post}/e_{i-1}^{prior}$. Then we update the prior emissions at time i as $e_i^{prior} = S_{i-1} \cdot e_i^{prior}$. This prescription enables us to derive spatial 2-D emission scaling factors which play the role of an emission forecast model."

- p13, l24: "Last but not least our results show that the information of wind uncertainties is not important for NOx emission estimation." I guess that the combined wind/NO2 analysis could also lead to adjustments of the winds which give a better match between observed NO2 concentrations and the location of the emission sources. The ensemble, with a spread equal to the wind uncertainty, would allow for such adjustments and could in principle outperform the system where the winds are prescribed. It seem the authors claim that such benefits are not significant?

In our OSSE system, a large volume of wind observations are assimilated to constrain wind in the boundary layer. Under such condition, the wind uncertainties are constrained under 1 m/s for most of the time and show peaks up to 1.5 m/s. Such uncertainties are too small to affect chemical assimilation performance as we find little difference in the emission estimation between ENS.1 and REA. We agree on the comment that the adjustment of the winds could benefit the comparison of observed NO_2 concentrations. However, in this assimilation system the wind uncertainties are constrained by wind observations only. With an ensemble of wind, the covariance between wind and NO_2 concentrations can potentially provide useful information to adjust winds. Such covariance is not used in ENS.1 as we only allow wind observations to affect wind analysis. In regards to the adjustment of wind from combined wind/NO_2 analysis, we will further discuss this in our next paper. In addition, this issue does not conflict with our current finding on the impact of wind uncertainties on NO_x emission estimation. We modified the text as below:

"We would like to point out that the covariance of error statistics between wind and NO_2 are not utilized in the OSSE assimilation in this paper. Results on carbon and weather assimilation show that the variable localization scheme we use zeroes out the background error covariance among prognostic variables that are not physically related, thus reducing sampling errors (Kang et al., 2011). Specifically, they find that covariance between carbon fluxes and meteorological variables should be neglected. However, the same result might not obtain for short-lived chemicals. The extent to which chemical observations can be used to improve the assimilation of meteorological variables and vice-versa in a situation where we do not zero the covariance in the errors should be pursued in future research."

- p13, l26: "Assimilations of NO₂ only with the meteorology constrained from an hourly weather assimilation product would perform as well as the joint assimilation of meteorology and chemistry."

Do you suggest that a CTM with prescribed meteorological analyses will perform as well as a fully integrated chemistry-meteorology analysis system?

We draw such conclusions based on our OSSE result with specific setup options. One important treatment in our OSSE is that we exclude the interaction between chemistry and meteorology during the filtering step. Under this condition, the ensemble statistics between chemistry and meteorology in the integrated chemistry-meteorology assimilation system is not utilized. Our results show that a CTM with prescribed meteorological analyses performs as well as such an integrated system. We modified the text in the response to the previous comment.

- p13, l34: "will fail" -> will also fail

We updated the text as below:

"However, an approach that didn't work in the ideal case will also fail in the realistic scenario with spatially-inhomogeneous emission perturbations."

References:

Kang, J.-S., Kalnay, E., Liu, J., Fung, I., Miyoshi, T. and Ide, K.: "Variable localization" in an ensemble Kalman filter: Application to the carbon cycle data assimilation, J. Geophys. Res., 116(D9), D09110, doi:10.1029/2010JD014673, 2011.

Assimilation of satellite NO$_2$ observations at high spatial resolution using OSSEs

X. Liu[1], A. Mizzi[2], J. Anderson[3], I. Fung[1] and R.C. Cohen[1,4]

[1]Department of Earth and Planetary Science, University of California at Berkeley, Berkeley, CA, USA
5 [2]Atmospheric Chemistry Observation and Modeling Laboratory, National Center for Atmospheric Research, Boulder, CO, USA
[3]Institute for Mathematics Applied to Geosciences, National Center for Atmospheric Research, Boulder, CO, USA
[4]Department of Chemistry, University of California at Berkeley, Berkeley, CA, USA

10 *Correspondence to*: Ronald C. Cohen (rccohen@berkeley.edu)

Abstract. Observations of trace gases from space-based instruments offer the opportunity to constrain chemical and weather forecast and reanalysis models using the tools of data assimilation. In this study, Observing System Simulation Experiments (OSSEs) are performed to investigate the potential of high space and time resolution column measurements as constraints on urban NO$_x$ emissions. The regional chemistry-meteorology assimilation system where meteorology and chemical variables are simultaneously assimilated is comprised of a chemical transport model, WRF-Chem, the Data Assimilation Research Testbed and a geostationary observation simulator. We design OSSEs to investigate the sensitivity of emission inversions to the accuracy and uncertainty of the wind analyses and the emission updating scheme. We describe the overall model framework and some initial experiments that point out first steps toward an optimal configuration for improving our understanding of NO$_x$ emissions by combining space-based measurements and data assimilation. Among the findings we describe are the dependence of errors in the estimated NO$_x$ emissions on the wind forecast errors, showing that wind vectors with root mean standard error (RMSE) below 1 m/s allow inference of NO$_x$ emissions with RMSE less than 30 mol/(km^2·hr) at the 3 km scale of the model we use. We demonstrate that our inference of emissions is more accurate when we simultaneously update both NO$_x$ emissions and NO$_x$ concentrations instead of solely updating emissions. Further, based on our analyses, we recommend carrying out meteorology assimilations to stabilize NO$_2$ transport from the initial wind errors before starting the emission assimilation. We show that wind *uncertainties* (calculated as a spread around a mean wind) are not important for estimating NO$_x$ emissions when the wind uncertainties are reduced below 1.5 m/s. Finally, we present results assessing the role of separate vs. simultaneous chemical and meteorological assimilation in a model framework without covariance between the meteorology and chemistry.

30

1 Introduction

Weather and climate act in concert with emissions to establish the concentrations of chemicals and aerosols in the boundary layer. To understand the factors that affect public health and the productivity of agriculture and animal husbandry, we require accurate models of both emissions and the boundary layer meteorology to define the surface layer concentrations that determine the exposure of humans, animals and plants to chemicals and aerosol. There remain substantial uncertainties in even the best models of emissions and even more so in the best models of boundary layer dynamics (for example, Hu et al., 2010). Current uncertainties in the surface NO_2 emission inventories in the U.S. are thought to be of order 50% (Krotkov et al., 2016; Travis et al., 2016). Comparable uncertainties affect estimates of the planetary boundary layer (PBL) height and mixing rates that redistribute emissions from the surface (Kretschmer et al., 2012, 2014; Lauvaux and Davis, 2014).

Over the last decade, there has been increased use of data assimilation techniques to constrain model forecasts and reanalyses of atmospheric constituents (e.g. Arellano Jr. et al., 2007; Edwards et al., 2009; Claeyman et al., 2011; Lahoz et al., 2012; Pagowski and Grell, 2012; Bowman, 2013; Gaubert et al., 2014; Hache et al., 2014; Saide et al., 2014; Zoogman et al., 2014; Barré et al., 2015; Bousserez et al., 2016; Mizzi et al., 2016). Assimilation of chemicals can be extended to optimize model inputs, such as emissions thereby providing insight into how to improve the processes that govern the model performance (e.g. Elbern et al., 2007; Barbu et al., 2009; Chatterjee et al., 2012; Miyazaki et al., 2012b; Koohkan et al., 2013; Yumimoto, 2013; Cui et al., 2015; Guerrette and Henze, 2015; Turner et al., 2015).

To date most efforts to incorporate satellite remote sensing in data assimilation have focused on long-lived chemicals such as CO, CH_4 or CO_2 and regional and continental scale aspects of emissions. Processes that govern variability of emissions within an urban center require new approaches that use high spatial and temporal resolution models and observations. NO_2 has a lifetime of only a few hours and thus exhibits concentration changes that are substantial on spatial scales of 50-75 km. Observations of variations in NO_2 are thus uniquely suited to study emissions and meteorology at the scales of cities. Averaged measurements of NO_2 have been shown to be promising for evaluation of absolute emissions and trends (Russell et al., 2012; Miyazaki et al., 2016) as well as providing information on the coupling of boundary layer winds to chemical lifetime (Beirle et al., 2011; Valin et al., 2013). Current space based instruments have resolution that is too low to provide direct information on lifetimes and emissions from a single overpass. Instead, analyses have focused on averages of the data that wash out some of the key details about emission location and chemical lifetime.

New instruments with spatial resolution of a few kilometers will soon change that situation. The TROPOspheric Monitoring Instrument (TROPOMI, launch date mid 2017) will be the first to provide spatial resolution sufficient to observe these NO_2 changes on a single overpass. TROPOMI will view the atmosphere from low earth orbit and provide one image per day. We also anticipate the launch of three geostationary satellites, the Geostationary Environmental Monitoring Spectrometer (GEMS), the Tropospheric Emissions: Monitoring of POllution (TEMPO) and Sentinel-4, which will provide observations at

higher temporal resolution with hourly repeat at locations in Asia, North America and Europe, respectively (Zoogman et al., 2017). The spatial resolution of these new low earth orbit (LEO) and Geostationary (GEO) instruments will be sufficient to provide ~10 samples within the advection distance that is determined by the chemical lifetime of NO_2. This dense sampling will permit characterization of multi-exponential or non-exponential behavior where current analyses are typically forced to assume single exponential decay. To take full advantage of these measurements within a data assimilation system, we will need to model the NO_2 column at similar spatial resolution. This is both because the spatial scales of important variation in atmospheric plumes are on the order of 4 km and because of the steep non-linearity in the lifetime of NO_2 as a function of the NO_2 concentration. For example, biases of 34% (3.3 to 5.0×10^{15} molecules/cm^2) are found in the modeled averaged NO_2 column over Los Angeles at resolutions of 96 km compared to 12 km. For a point source, such as a power plant, model convergence is observed only at a grid resolution of 4 km or smaller (Valin et al., 2011).

In this study, we describe a high spatial and temporal resolution chemical transport ensemble data assimilation system with joint assimilation of meteorology and chemistry to adjust NO_x emissions on scales consistent with the temporal scale of NO_x evolution. We use that forecast/assimilation system to investigate the factors that influence the capability of TEMPO NO_2 observations to accurately constrain NO_x emissions. Our long-term goal is to estimate hour-to-hour variations in NO_x emissions at the scale of model grid point resolution (3 km) and to use these variations to understand the processes controlling the emissions. The remainder of this paper is organized as follows: In section 2, we describe the forecast/data assimilation system, the system setup, observations, and the TEMPO NO_2 simulator – the simulation of column NO_2 that would be observed by TEMPO. In section 3, we describe the experimental design including a series of assimilation experiments that guide optimization of the emission estimation performance. In section 4, we assess the performance of meteorology and chemistry assimilation. We then discuss the results and provide insight into the potential accuracy of NO_2 emission fields derived from geostationary NO_2 observations. We conclude in section 5.

2 The data assimilation system

The forecast/data assimilation system used here is WRF-Chem/DART as described by Mizzi et al. (2016). It consists of the following elements: the forecast model, the assimilation engine, and observations of meteorological and chemical states to be assimilated.

2.1 WRF-Chem model description

The core meteorological and chemical forecast model is the regional online CTM WRF-Chem v3.4.1 (www2.acd.ucar.edu/wrf-chem). The model domain is a one-way nest with an outer domain of 12 km resolution covering western North America and an inner domain of 3 km resolution focused on the city of Denver, CO (Figure 1). The 3 km domain is 660 km by 840 km. The model has 30 vertical levels between the surface and an upper boundary of 100 mb and 10 levels within the boundary layer (~1.5 km). Simulations of meteorology on the outer domain are initialized and constrained

at the lateral boundary by North American Regional Reanalysis (NARR) data from National Centers for Environmental Prediction (NCEP). The NARR data have a native horizontal resolution of 32 km with 45 pressure levels and 3 h temporal resolution. We use the global chemical model output from MOZART to initialize the chemical simulation on the outer domain and to provide the chemical boundary condition. After a spin-up time of four days on the outer domain, the inner

5 domain simulation is initialized and constrained through one-way nesting in both meteorology and chemistry.

Anthropogenic emissions for WRF-Chem are from the National Emission Inventory (NEI) 2011 Version 1 at native 4×4 km^2 resolution. The NEI 2011 provides hourly-varying emission for a typical weekday in summertime. The emissions do not vary from day to day. Biogenic emissions are calculated online with the simulation results by Model of Emissions of Gases and Aerosols from Nature (MEGAN). Fire emissions are not included. We use the widely-used regional acid deposition

10 model version 2 (RADM2) as the gas phase chemical mechanism (Stockwell et al., 1990). There are 59 species and 157 reactions to represent both inorganic and organic chemical reactions under tropospheric conditions. It includes the chemical losses of NO$_x$ through reaction with OH radical to form nitric acid, and other NO$_x$ sinks as peroxyacyl nitrates and alkyl nitrate.

2.2 DART ensemble assimilation system

15 WRF-Chem/DART is a regional multivariate data assimilation system developed by the National Center for Atmospheric Research (NCAR) to analyze meteorological variables and chemical variables simultaneously (Mizzi et al., 2016). We use the Ensemble Adjustment Kalman Filter (EAKF) in DART to analyze the states with an ensemble size of 30. Details of the EAKF algorithm and its implementation in DART are documented in (Anderson, 2001; Anderson and Collins, 2007; Anderson et al., 2009). In this study the system is extended to assimilate synthetic TEMPO NO$_2$ column observations. As

20 emissions are not prognostic variables of the forecast model, we implement a state augmentation approach to include emissions in the state variables (Aksoy, 2006). The chemical state variables include the NO$_2$ concentration, NO$_x$ emissions. The meteorological state variables are U, V, W, T, QVAPOR, QCLOUD, QRAIN, QICE, QSNOW (MU and PH are used in vertical coordinate transforms, T2, Q2, U10, V10, PSFC used for surface data assimilation forward operators.) based on the settings used in meteorology data assimilation. Definitions of these variables are taken from Romine et al. (2013), and are

25 given in the Appendix. Adaptive spatially and temporally varying inflation is applied to the prior state to assist in maintaining the ensemble spread. We summarize the DART configuration details in Table 2.

2.2.1 Spatial localization

In ensemble methods the correlations among spatially remote variables in the prior ensemble are regarded as spurious correlations due to the small ensemble size (30). To compensate for this under-sampling issue, spatial localization is

30 introduced to reduce the prior correlations based on the distance between the observed/modeled state variables (Houtekamer and Mitchell 2001). In this study, we apply the fifth-order distance-dependent Gaspari and Cohn (GC) function (Gaspari et al., 1999) to reduce the spurious impact of observations on spatially remote state variables. The scaling distance in the GC

function is defined by a half-width parameter, two times which is the distance where the GC function goes to zero. With a data assimilation window of one hour and a maximum wind speed of 3~5 m/s, an observation of column NO_2 primarily reflects information about emissions that occurred during the last hour and within 10 km. We use the half-width distance in spatial localization as 10 km and demonstrate this as the optimal value based on sensitivity experiments with localization distances of 5 km, 10 km, 20 km and 50 km. Because of the high density of TEMPO NO_2 observations (2×4.5 km^2), the update of chemical state variables is mostly determined by the local observations.

2.2.2 Variable localization

Similar to the concept of spatial localization, variable localization techniques have been introduced (Arellano Jr. et al., 2007) to reduce spurious correlations among observations and different types of state variables. For example, for CO_2 flux estimation, Kang et al. (2011) showed that the performance of data assimilation using a variable localization that zeros out the prior error covariance between meteorological variables and CO_2 flux is better than using a standard full covariance approach. Here we isolate the influence of meteorological observations on chemical variables and vice versa.

2.3 Initial and boundary condition ensemble

We generate the initial chemical ensemble by adding the perturbations to the mean state of the fine domain forecast. In the ensemble method the generated ensemble should represent the error statistics of the initial guess of the model state (Evensen 2003). The correlation between perturbations of chemical state variables is modeled by a simple isotropic exponential decay function with a characteristic correlation length of 50 km. For the meteorology ensemble, random perturbations were added to each member by sampling the NCEP background error covariance using the WRF Data Assimilation System (http://www2.mmm.ucar.edu/wrf/users/wrfda) (Barker et al., 2012). The options used for the WRFDA settings are summarized in Table 3. The parameter cv_option indicates the background error options in WRFDA. With cv_option = 3, we use the NCEP background error covariance, which is estimated in grid space by what has become known as the NMC method. The statistics are estimated with the differences of 24 and 48-hour GFS forecasts with T170 resolution, valid at the same time for 357 cases, distributed over a period of one year. The parameter je_factor is the ensemble covariance weighting factor. This factor controls the weighting component of ensemble and static covariances. The ensemble member lateral boundary condition perturbations are generated in a similar manner as the initial ensemble using the fixed-covariance perturbation technique. The boundary condition for the analysis time is adjusted to match the analysis from DART. The tendencies for the later times in the forecast are adjusted to match the change in the boundary condition for the analysis time.

2.4 Emission update scheme

By including emissions in the ensemble state vector, emissions are estimated as hourly evolving parameters. Estimation of time-evolving emissions using data assimilation was first presented for carbon flux estimation (Kang et al., 2011, 2012). Such an approach provides emission information beyond an average for a specific time period. NO_x emissions within cities

show significant variation within the urban core and between the urban core and the surrounding suburbs. The observed columns show strong spatial variation dominated by an emission hotspot that results from the combination of spatial patterns in emissions and the short chemical lifetime. The goal of this work is to constrain hourly evolving emissions at the native model resolution. Here we start with a simple case in which the emission error is a constant fraction at all times of day with

5   the prior emissions set as 70% of the truth and we investigate the ability of assimilation to recover the original emissions.

A challenge for updating the emissions in the augmented state vector is the absence of an emission forecast model to evolve the emission variables forward in time. The bottom-up inventory to be optimized provides hourly-resolved emissions for each model grid point. Instead of treating the emission variables of each hour at a specific location as independent parameters, we update the emission scaling factors at each assimilation cycle. In our emission update scheme, the TEMPO

10   NO_2 observations at time i are assimilated to generate a scaling factor for emissions at time i-1. In this way, the model-observation difference in the NO_2 column will correct the emission of an hour ago instead of the current emission. This approach is reasonable because errors in NO_2 concentration result from errors in previous emissions. Considering the short NO_2 lifetime of three hours in summer daytime, emissions from the previous hour have a large contribution to the NO_2 total mass at the current time. For a given model grid point, we define the emissions of truth (e_{i-1}^t), prior (e_{i-1}^{prior}) and posterior

15   (e_{i-1}^{post}) at time $i-1$. Since we start the assimilation with 70% of true emissions, we have $e_m^{prior} = 0.7e_m^t$ for any time m. After assimilating observations at time i, we compute the scaling factor (S_{i-1}) for emissions at time $i-1$ as follows: $S_{i-1} = e_{i-1}^{post}/e_{i-1}^{prior}$. Then we update the prior emissions at time i as $e_i^{prior} = S_{i-1} \cdot e_i^{prior}$. This prescription enables us to derive spatial 2-D emission scaling factors which play the role of an emission forecast model.

2.5 Synthetic meteorological and chemical observations

20   Observations assimilated include meteorological observations and NO_2 column retrievals from the TEMPO OSSE. For meteorological observations, we assimilated synthetic observations of temperature, wind and humidity from the NCEP Meteorological Assimilation Data Ingest System (MADIS) (https://madis.noaa.gov/). MADIS is a meteorological observational database and data delivery system that provides observations that cover the globe. MADIS ingests data from NOAA data sources and non-NOAA providers, decodes the data then encodes all of the observational data into a common

25   format with uniform observational units and time stamps. For wind observations, the assimilated observation types include standard aviation routine weather report (METAR), wind profilers, aircraft-based observations (ACARS), national mesonet data and satellite data. Among them the mesonet wind data is the most abundant with ~1000 observations located in the mapping domain in Figure 2. The observation errors are the default values from the DART facility that are defined based on NCEP statistics (Romine et al., 2013)

30   The GEOstationary Coastal and Air Pollution Events (GEO-CAPE) mission (Fishman et al., 2012) aims at improving our understanding of both coastal ecosystems and air-quality from regional to continental scales. As the first phase of the GEO-CAPE implementation, TEMPO (Zoogman et al., 2017), launch date circa 2019, will provide hourly measurements of NO_2,

HCHO, tropospheric ozone, aerosols, and cloud parameters during the daytime. TEMPO will measure solar back scattered light in the UV-Vis spectral range. Implemented on a geostationary platform, TEMPO retrievals will achieve hourly observations of NO_2 vertical column density (VCD) at a native spatial resolution of 2×4.5 km during the day-lit period. TEMPO's high spatiotemporal resolution will allow a more detailed assessment of emission inventories, e.g. urban scale and

5 large power plant NO_2 emissions and mobile emissions that show significant spatial and temporal variations due to urban transit patterns, than is possible with existing LEO observations.

As the TEMPO has not been launched yet, we generate synthetic TEMPO NO_2 observations by simulating the instrument's observing characteristics. We carried out a model run, i.e. a forward integration of WRF-Chem for the period from July 2nd to July 7th 2014 with NO_2 emissions specified by NEI 2011 ('truth'). In the NO_2 retrieval algorithm, a layer dependent Box-

10 Air Mass Factor (BAMF) represents the sensitivity of the retrieved NO_2 in a specific layer to the true value in the atmosphere. The BAMF of NO_2, as an optically thin absorber, is a vector and determines the measurement sensitivity to NO_2 molecules at 35 pressure levels. In the calculation of BAMFs, we follow the latest version of the NASA standard product retrieval (Level 2, Version 2.1, Collection 3) algorithm (Bucsela et al., 2013) assuming the TEMPO measurement has similar characteristics to OMI. We assume clear-sky conditions for all observing scenes. Cloudy-sky scenes affect only the number

15 of observations available as the cloudy scenes are usually discarded in the data filtering process. Without running a radiative transfer code, the elements of the BAMF vector are computed as a function of solar zenith angle (SZA), viewing zenith angle (VZA), relative azimuth angle (RAA), terrain reflectivity (Rt), terrain pressure (Pt), atmospheric pressure level, (p) and the NO_2 profile (Bucsela et al., 2013). The viewing parameters are computed by simulating the viewing geometry based on the location of ground pixels in relation to the observing instrument. The geometry related parameters (SZA, VZA and RAA) are

20 computed hourly for each TEMPO observation using Matlab functions sun_position.m and geodetic2aer.m with inputs of the location and time of each TEMPO observation, and the location (36.5°N, 100°W) and altitude (35,786 km) of the TEMPO sensor. The terrain reflectivity and terrain pressure are sampled from the WRF-Chem nature run (NR, see section 3) for each TEMPO pixel. All the parameters have an hourly frequency consistent with the TEMPO temporal observing pattern. Consequently, the NO_2 profile with high-spatial-temporal resolution captures the diurnal variation of NO_2 and its urban-rural

25 contrast. This contrast is essential to accurate interpretation of the measured spectrum (Russell et al., 2011; Laughner et al., 2016).

To generate synthetic TEMPO data, the modeled 3-D concentration fields from the NR are sampled in as similar a manner to the planned TEMPO measurements as the transport model permits: using the computed BAMF vertically; hourly frequency; 2×4.5 km nadir resolution and variations following the Earth's curvature horizontally. Figure 2 shows an example of the

30 spatial distribution of TEMPO data over Denver, CO.

We describe the observation error as a relative value (σ_{rel}) and a random draw from a Gaussian distribution to avoid using a fixed value. The magnitude of the relative mean uncertainty of the NO_2 column is different between clean and polluted areas (Boersma et al., 2004). We follow their categorization of clean versus polluted regions and summarize the mean and standard deviation of a Gaussian distribution for each scenario in Table 4. For polluted regions, we give mean uncertainty of

7.5%, which is lower than the 35% minimum in the OMI NO_2 retrievals. First, most of these errors are systematic affecting comparison of different cities but have smaller variation across a single, small area scene of observations. Second, a relatively lower observation error improves the efficiency of data assimilation and helps to examine the sensitivity to other parameters. Finally, as TEMPO is expected to be operational no sooner than 2018, it is reasonable to expect the retrieval error which is dominated by the air mass factor (AMF) in regions with large columns will be reduced as a result of future improvements in AMF simulation (Laughner et al., 2016). The synthetic observations assimilated are obtained by sampling the NR using the TEMPO observation simulator and adding observation error as $y^{obs} = N(y^{tr}, \sigma^2)$, where y^{tr} is the TEMPO NO_2 observations sampled from the truth, and σ is the observation error standard deviation computed as $\sigma = y^{tr} \cdot \sigma_{rel}$.

3 Assimilation experiments

We begin by performing OSSEs in the context of a perfect model. The original NEI 2011 is used as the emission input for the NR without any emission perturbation. We consider the NR as the true atmosphere and sample meteorological and NO_2 observations from the NR. The control run (CR) is a parallel model calculation to the NR and suffers from imperfect model input and parametrization. The differences between the NR and the CR in this study are the emission inputs and the initial conditions for the meteorology. We begin by creating a NR and a CR simulation on the outer domain of 12 km resolution (d01) without assimilating observations using a simulation setup as described above in section 2.1. We impose a difference to the CR by using emissions in the CR that are scaled to be 70% of the NR emissions. We apply the identical forecast model (WRF-Chem) for both the NR and the CR to isolate the behavior of the ensemble filter algorithm from the influence of the model errors. Then the NR and the CR on the inner domain of 3km (d02) are initialized from the corresponding d01 simulations respectively on 06:00 local time (LT) on July 2nd 2014. At the time of initialization, the NR and CR on d02 share the same meteorological fields and differ in NO_x concentrations due to different emission inputs. Our next step is to generate a 30-member ensemble from the CR. We use WRFDA to generate an ensemble in meteorological variables (Barker et al., 2012). For chemical states, we give an ensemble in NO_x emissions and concentrations using the method described above in section 2.3. The forecast of the CR ensemble is the prior estimate of the states and will be combined with the observations in the assimilation cycle to yield the posterior states. By comparing the posterior emissions with the "true emission", we evaluate the data assimilation performance. We run assimilation experiments from 10:00 LT 2014/07/02 to 18:00 LT 2014/07/05 with an assimilation window of one hour. We assimilate ~20,000 weather observations in each assimilation window and ~9,000 TEMPO NO_2 column observations in each daytime assimilation window.

We design a series of experiments to explore the optimal approach to estimate NO_x emissions as shown in Table 1. In all experimental runs, we bias the CR initial emissions to be 30% below the reference emissions and examine the ability of the assimilation to recover the reference emissions. First, a reference assimilation run (REF) is conducted without including the meteorological ensemble so that the NR and CR ensembles have identical meteorological simulations. This shows the best

case scenario to constrain emissions assuming no errors associated with meteorology. In practice, the modeled meteorology is different from the true atmosphere due to errors in the model initial conditions, parameterizations and resolutions. In a more realistic simulation case labelled as ENS, we initialize both the meteorology and the NO_x emissions using an ensemble in which both weather observations and TEMPO NO_2 columns are assimilated. In ENS.1 the CR ensemble is generated by adding perturbations to the CR mean state. In this example, the CR ensemble mean meteorology is very close to the NR because CR and NR differ in NO_x emissions only. For the chemistry, the assimilated TEMPO NO_2 observations are allowed to update both the NO_2 concentration and the NO_x emissions every hour. In ENS.2 we allow NO_2 observations to update NO_x emissions but not the NO_x concentrations and keep the meteorology assimilation the same as ENS.1. By comparing ENS.1 and ENS.2 we evaluate the additional benefits of updating concentrations when observations are assimilated to constrain emissions. In ENS.3, we use the meteorology of the next day to initialize the CR ensemble so that there is some difference between the CR ensemble mean and the NR in the meteorology. To be specific, the CR meteorology ensemble on 2014/07/03 9:00 LT is used as the CR ensemble on 2014/07/02 9:00 LT. This is to mimic our imperfect knowledge of the atmospheric state and its uncertainty. ENS.1 and ENS.3 differ only in the meteorology of the initial ensemble. By comparing these two runs, we evaluate the sensitivity of the NO_2 assimilation to the initialization of the meteorology. Our final experiment REA mimics a general approach to a chemistry-only data assimilation where the meteorology is extracted from an existing reanalysis. REA reinitializes the meteorological state every hour with the best estimate of meteorological states generated by ENS.1. By design, REA has a single run of meteorology but uses an ensemble of NO_2 emissions and concentrations that are affected by assimilation of TEMPO NO_2 observations. As in ENS.1, REA includes simultaneous updates to emissions and concentrations.

4 Results

We evaluate the assimilation result by comparing with the NR states. We calculate the root mean square errors (RMSE) of observed quantities by $\sqrt{\sum_i^n (y_i^m - y_i^t)^2 / n}$, where y_i^m and y_i^t are the model and true values for the ith observation respectively, and n is the total number of observations of interest. We also calculate the RMSE of model states by $\sqrt{\sum_i^n (x_i^m - x_i^t)^2 / n}$, where x_i^m and x_i^t are the model and true states at the ith model grid point respectively, and n is the total number of grid points of interest. For the wind variable, the grid points of interest are all the points located within a sub-model space as shown in Figure 2, containing the lowest 10 model levels vertically. Because NO_x is located mostly in the boundary layer, the NO_2 transport error is determined by the meteorological errors in the lowest 10 model levels. For NO_x emission variables, the grid points of interest are categorized as emission points with emissions greater than 50 mol/(km^2·hr). Our analysis does not include emissions below 50 mol/(km^2·hr) because the observations over such low emission regions have large uncertainty and are not constrained. We also analyze the uncertainty of the prior and posterior estimates. The uncertainty is expressed by the 1-σ standard deviation of the ensemble.

4.1 Wind assimilation

The success of ensemble-based assimilation relies on how well the ensemble system represents the uncertainty. One way to test the success of an OSSE is to compare the RMSE computed with respect to the "true" observations with the ensemble spread directly. Figure 3 shows the evolution of the RMSE and spread for mesonet observations of zonal wind for ENS.1 and ENS.3. Overall, for each experiment the variation and magnitude of prior ensemble spread are similar to those of the prior RMSE, indicating that the ensemble develops a good amount of spread for the success of OSSE.

We find the errors in the observation space of mesonet winds are reduced by 50% on average from the prior to the posterior. The prior wind RMSE exhibits peaks in the afternoon and this results in the largest error reduction. The posterior wind RMSE shows a temporal average of 0.39 m/s and 0.47 m/s in ENS.1 and ENS.3 respectively. Because ENS.1 is initialized with a meteorology ensemble with its mean close to the truth, the wind RMSE on the first day is low and gradually grows to about 1 m/s. In contrast, the prior wind RMSE in ENS.3 is as high as 2 m/s on the first day as a result of using an initial meteorology ensemble that is very different from the truth. The wind RMSE evolution in the two experiments becomes very similar after the afternoon of the third day of assimilation, 2014/07/04. We conclude that the ensemble wind assimilation system performance is independent of the initialization approach after the first day.

4.2 TEMPO NO$_2$ assimilation

We assimilate hourly TEMPO NO$_2$ column observations and take their difference with the modeled column to correct the predicted NO$_2$. Figure 4 shows the TEMPO NO$_2$ column RMSE evolution for all experiments. With perfect knowledge of meteorology, REF shows significant reduction in TEMPO NO$_2$ RMSE in the first three update cycles, and succeeds in recovering the true emissions (Figure 5). The prior TEMPO NO$_2$ RMSE in the last three days varies below 3×10^{14} molecules/cm^2 as a result of perfect NO$_2$ transport and improved emissions. This ideal case with the assumption of perfect meteorology sets the upper limit of error reduction in NO$_2$ concentrations by assimilating the TEMPO NO$_2$ observations. Compared with REF, ENS.1 shows prior TEMPO NO$_2$ RMSE of $5\sim10\times10^{14}$ molecules/cm^2 due to the errors in NO$_2$ transport and emissions. By assimilating NO$_2$ observations, the TEMPO NO$_2$ RMSE is reduced by more than 50% from the prior to the posterior indicating the potential of TEMPO NO$_2$ observations to improve the modeled atmospheric NO$_2$ composition for the chemical reanalysis product. Without updating the NO$_2$ concentrations in ENS.2, there is no reduction in the TEMPO NO$_2$ RMSE as expected. We find the TEMPO NO$_2$ RMSE varies above 1×10^{15} molecules/cm^2, being the largest among all experiments because the emission estimations show very poor results (shown in section 4.3). The TEMPO NO$_2$ RMSE development in ENS.3 is very similar to ENS.1 except for the first day when ENS.3 shows higher errors in the wind field, which contribute to the NO$_2$ transport errors. We find the NO$_2$ forecast using a single meteorology field in REA is very similar to the ensemble NO$_2$ forecast in ENS.1. This is because there is very little difference between the one-hour meteorology forecast and the ensemble forecast. In addition, the emission estimation results are also very similar. This is different from the previous study on CO$_2$ forecasts which showed that for a 6-hour forecast, the CO$_2$ transport driven by a

single meteorological field has weaker vertical mixing and a stronger CO_2 vertical gradient when compared to the mean of the ensemble CO_2 forecasts initialized by the ensemble meteorological field (Liu et al., 2011).

We compare the TEMPO NO_2 column spread in REF and ENS.1 in Figure 6. For both experiments, the prior NO_2 column spread varies with a magnitude that is similar to the prior RMSE (Figure 4), which is the range desired for the NO_2 ensemble
5 spread. The NO_2 forecast uncertainty represented by the NO_2 ensemble spread results from the uncertainties in NO_2 transport and emissions since the uncertainties in chemical production and removal processes are not included in this study. The uncertainties in NO_2 transport are determined by the prior wind ensemble spread, which is widest in the afternoon and stays as low as ~ 0.5 m/s at other times for zonal wind (Figure 3). The prior NO_x emission uncertainties are 60% after inflation (Figure 5). Under these circumstances, the mean prior TEMPO NO_2 column spread is 4.55×10^{14} molecules/cm^2 in REF
10 which does not include NO_2 transport uncertainties, and is 7.03×10^{14} molecules/cm^2 in ENS.1 which takes uncertainties in transport and emissions into account. The difference indicates that NO_2 transport contributes to 35% of the total NO_2 forecast uncertainties in our assimilation setup. The TEMPO NO_2 column spread in REF is very stable because it is determined by the constant emission spread of 60%. ENS.1 shows fluctuations in the evolution of TEMPO NO_2 column spread which corresponds to the wind spread variation with increasing spread in the afternoon.

15 **4.3 NO_x emission estimation**

We show the time evolution of the averaged urban emissions for all experiments in Figure 5. For all experiments, the posterior emission ensemble spread is reduced compared to the prior spread, suggesting the effectiveness of assimilated NO_2 columns in constraining the emission uncertainties. In making these comparisons, we ignore the emission correction of the first assimilation cycle, since the first update produces a significant over-correction to emissions because of the accumulated
20 underestimation of the NO_2 concentrations. By neglecting the first update, the prior emission ensemble mean of the second cycle is still 70% of the truth. During the nighttime when TEMPO observations are not available, we calculate the ratio of posterior ensemble mean to the truth in the last cycle of daytime and use this together with the nighttime true emissions to derive the ensemble mean for the nighttime emissions. The prior and posterior emission ensemble of each nighttime hour is the same.

25 Not surprisingly, under the condition of perfect knowledge in meteorological fields, assimilating TEMPO NO_2 observations successfully improves the emissions within the first few updates. The estimated emissions agree well with the true emissions throughout the assimilation period. This demonstrates the capability of a geostationary NO_2 column observing system to constrain city-scale emissions and the reliability of the ensemble-based assimilation method to project the observed information to emissions.

30 We find the errors in estimated emissions correlate with the wind errors. In ENS.1, the posterior emission is corrected to the truth at the second cycle and stays close to the truth throughout the first day. The good performance on the first day benefits from an initial meteorology ensemble with its mean close to the truth. For the following three days, the emission estimates succeed in recovering the true emissions during the morning and show deviations from the truth in the afternoon as a result

of the increased error in boundary layer winds. Figure 7 shows the dependence of errors in the inverted emissions to the prior wind RMSE. The emission errors show high sensitivity to the wind errors with the slope of the regression line of 32.5 mol·km^{-2}hr^{-1}/(m·s^{-1}). With the RMSE of model predicted wind vectors of 1 m/s, the errors in the estimated emissions are 30 mol·km^{-2}hr^{-1} on average. For the daytime cycles, the prior emission ensemble spread after inflation is approximately 60%
5   and is reduced by more than half after assimilation (Figure 5). Even though the posterior ensemble mean does not match with the truth in the afternoon, the truth falls within the range of the posterior ensemble spread with a few exceptions.

We find the simultaneous update of emission and concentration performs better than the emission update only scheme with an hourly assimilation window. ENS.2 is a parallel assimilation run with ENS.1 but updates emissions only. As shown in Figure 5, the estimated emissions have very large differences from the truth and the posterior ensemble spread does not
10   cover the truth. For example, at 10:00 July 3rd, the posterior ensemble mean (red) is very close to the truth. As a result of this, we have a very good prior ensemble estimate (black) at 11:00. However, the posterior emission at 11:00 is largely underestimated compared with the truth. This is because the posterior emissions from 7:00 to 9:00 are overestimated which results in overestimated NO$_2$ concentrations at 10:00 and 11:00. As a result, even though the prior emissions from 10:00 to 11:00 are good, the model still overestimates NO$_2$ at 11:00 due to the NO$_2$ overestimation at 10:00. Without updating the
15   concentrations, the observed differences in NO$_2$ columns are dominated by the NO$_2$ concentration errors of an hour ago and should not be attributed to the emissions.

We also find that the emission estimation should start after the meteorology assimilation becomes stable. As a comparison to ENS.1, ENS.3 is initialized with a meteorology ensemble that is very different from the truth. On the first day, the prior wind RMSE varies from 1 m/s to 2 m/s (Figure 3) and leads to enhanced NO$_2$ transport errors. As a result, the emission
20   estimations are not successful for the first day. After the afternoon of the second day (07/03), the wind RMSE evolution is similar between ENS.1 and ENS.3 and as a result, the emission estimations perform in a similar way. We recommend allowing meteorology assimilations to stabilize from the initial transport errors before assimilating chemical observations to constrain the emissions.

With an hourly re-initialization of meteorology, the NO$_2$ transport error statistics are not important to emission estimation if
25   the current practice of using a single meteorological field to transport NO$_2$ is adopted. The emission estimation performance in REA is very similar with that in ENS.1 (Figure 5). This is because the difference in the one-hour NO$_2$ forecast driven by an ensemble meteorological field and a single ensemble mean field is very small. Though the wind uncertainties represented by the meteorological ensemble reach 1.5 m/s in the afternoon, our results show that the information of wind uncertainties is not important for estimating NO$_x$ emissions.
30   Finally we examine the emission estimation performance in ENS.1 at the scale of the model grid (3 km). As shown in Figure 8, the true emission shows high spatial variation from city center to suburban as well as distinct point emission sources. In the example of the emission estimate at 9:00 am, the posterior emission recovers the truth very well with the posterior RMSE of 21.6 mol/(km^2·hr). In contrast, the emission estimate at 4:00 pm shows RMSE of 46.5 mol/(km^2·hr) due to relatively high wind errors. The posterior underestimates the emissions significantly all over the city except for the regional overestimation

in the east. The emission hot spot of ~250 mol/(km^2·hr) in the city center is not fully represented in the posterior estimate. In conclusion, when wind errors are low, the difference between posterior emission and the truth can be reduced to ± 25 mol/(km^2·hr) at most grid points. With high wind errors that difference varies significantly from point to point and grows as large as 100 mol/(km^2·hr).

5 Summary and conclusions

In this study, we explore an approach to estimate NO$_x$ emissions by assimilating column NO$_2$ and meteorological observations in system comprised of the regional CTM, WRF-Chem, and the DART-EAKF. This ensemble-based data assimilation system allows the flexibility to assimilate observations of meteorological and chemical variables on various space and time scales. Our approach anticipates the future availability of long-term, high spatial resolution, and frequent repeats of multiple species from satellites, such as TEMPO.

Previous work has shown that NO$_x$ concentrations and columns vary at fine scales necessitating high spatiotemporal resolution to make use of them in the assimilation. In the coupled chemical and meteorological data assimilation system, we apply an OSSE framework to estimate NO$_x$ emissions in Denver by jointly assimilating MADIS observation of meteorological variables as well as future TEMPO NO$_2$ columns. In the meteorological assimilation we successfully reduced the posterior wind RMSE below 0.5 m/s in Denver to better represent the NO$_2$ transport. The prior wind RMSE and spread show peaks in the afternoon thus increasing the errors in NO$_2$ transport. We find that the meteorological uncertainties contribute 35% to the total NO$_2$ forecast uncertainties considering the emission uncertainties of 60%. Assimilation of TEMPO NO$_2$ columns reduces errors in the predicted NO$_2$ concentration by more than 50%, which demonstrates the potential of future geostationary observations to constrain the NO$_2$ chemical weather.

One of the goals of this work is to investigate the optimal strategy to estimate NO$_x$ emissions. We test the upper limit of emission constraints from TEMPO NO$_2$ observations in an ideal case assuming no errors associated with the modeled meteorology. In the experiment of joint assimilation of meteorology and chemical NO$_2$, we find that the estimate of emissions is most successful in the morning but degrades in the afternoon when the prior wind RMSE grows above 1 m/s. Considering the dependence of errors in estimated emissions on the wind forecast errors, we recommend guaranteeing the accuracy in modeled wind and achieving wind RMSE below 1 m/s for the success of chemical assimilation to infer emissions at the 3-km scale of our model grid. We show that the simultaneous update of NO$_x$ emissions and concentrations outperforms the approach of updating emissions only. We recommend carrying out meteorology assimilations to stabilize from the initial transport errors before starting the emission inversion.

We would like to point out that the covariance of error statistics between wind and NO$_2$ are not utilized in the OSSE assimilation in this paper. Results on carbon and weather assimilation show that the variable localization scheme zeroes out the background error covariance among prognostic variables that are not physically related, thus reducing sampling errors (Kang et al., 2011). Specifically, they find that covariance between carbon fluxes and meteorological variables should be

neglected. However, the same result might not obtain for short-lived chemicals. The extent to which chemical observations can be used to improve the assimilation of meteorological variables and vice-versa in a situation where we do not zero the covariance in the errors should be pursued in future research.

10 **References**

Anderson, J., Hoar, T., Raeder, K., Liu, H., Collins, N., Torn, R. and Avellano, A.: The Data Assimilation Research Testbed: A Community Facility, Bull. Am. Meteorol. Soc., 90(9), 1283–1296, doi:10.1175/2009BAMS2618.1, 2009.

Anderson, J. L.: An Ensemble Adjustment Kalman Filter for Data Assimilation., Mon. Weather Rev. Dec2001, 129(12), 2001.

15 Anderson, J. L. and Collins, N.: Scalable Implementations of Ensemble Filter Algorithms for Data Assimilation, J. Atmos. Ocean. Technol., 24(8), 1452–1463, doi:10.1175/JTECH2049.1, 2007.

Arellano Jr., A. F., Raeder, K., Anderson, J. L., Hess, P. G., Emmons, L. K., Edwards, D. P., Pfister, G. G., Campos, T. L. and Sachse, G. W.: Evaluating model performance of an ensemble-based chemical data assimilation system during INTEX-B field mission, Atmos. Chem. Phys., 7(21), 5695–5710, doi:10.5194/acp-7-5695-2007, 2007.

20 Barbu, A. L., Segers, A. J., Schaap, M., Heemink, A. W. and Builtjes, P. J. H.: A multi-component data assimilation experiment directed to sulphur dioxide and sulphate over Europe, Atmos. Environ., 43(9), 1622–1631, doi:10.1016/j.atmosenv.2008.12.005, 2009.

Barker, D., Huang, X.-Y., Liu, Z., Auligné, T., Zhang, X., Rugg, S., Ajjaji, R., Bourgeois, A., Bray, J., Chen, Y., Demirtas, M., Guo, Y.-R., Henderson, T., Huang, W., Lin, H.-C., Michalakes, J., Rizvi, S. and Zhang, X.: The Weather Research and 25 Forecasting Model's Community Variational/Ensemble Data Assimilation System: WRFDA, Bull. Am. Meteorol. Soc., 93(6), 831–843, doi:10.1175/BAMS-D-11-00167.1, 2012.

Barré, J., Gaubert, B., Arellano, A. F. J., Worden, H. M., Edwards, D. P., Deeter, M. N., Anderson, J. L., Raeder, K., Collins, N., Tilmes, S., Francis, G., Clerbaux, C., Emmons, L. K., Pfister, G. G., Coheur, P.-F. and Hurtmans, D.: Assessing the impacts of assimilating IASI and MOPITT CO retrievals using CESM-CAM-chem and DART, J. Geophys. Res. Atmos., 30 120(19), 10,501–10,529, doi:10.1002/2015JD023467, 2015.

Beirle, S., Boersma, K. F., Platt, U., Lawrence, M. G. and Wagner, T.: Megacity emissions and lifetimes of nitrogen oxides probed from space., Science, 333(6050), 1737–9, doi:10.1126/science.1207824, 2011.

Boersma, K. F., Eskes, H. J. and Brinksma, E. J.: Error analysis for tropospheric NO 2 retrieval from space, J. Geophys. Res., 109(D4), D04311, doi:10.1029/2003JD003962, 2004.

Bousserez, N., Henze, D. K., Rooney, B., Perkins, A., Wecht, K. J., Turner, A. J., Natraj, V. and Worden, J. R.: Constraints on methane emissions in North America from future geostationary remote sensing measurements, Atmos. Chem. Phys. Discuss., 15(13), 19017–19044, doi:10.5194/acpd-15-19017-2015, 2015.

Bowman, K. W.: Toward the next generation of air quality monitoring: Ozone, Atmos. Environ., 80, 571–583, doi:10.1016/j.atmosenv.2013.07.007, 2013.

Bucsela, E. J., Krotkov, N. A., Celarier, E. A., Lamsal, L. N., Swartz, W. H., Bhartia, P. K., Boersma, K. F., Veefkind, J. P., Gleason, J. F. and Pickering, K. E.: A new stratospheric and tropospheric NO_2 retrieval algorithm for nadir-viewing satellite instruments: applications to OMI, Atmos. Meas. Tech., 6(10), 2607–2626, doi:10.5194/amt-6-2607-2013, 2013.

Chatterjee, A., Michalak, A. M., Anderson, J. L., Mueller, K. L. and Yadav, V.: Toward reliable ensemble Kalman filter estimates of CO2 fluxes, J. Geophys. Res. Atmos., 117(22), 1–17, doi:10.1029/2012JD018176, 2012.

Claeyman, M., Attié, J.-L., Peuch, V.-H., El Amraoui, L., Lahoz, W. A., Josse, B., Ricaud, P., von Clarmann, T., Höpfner, M., Orphal, J., Flaud, J.-M., Edwards, D. P., Chance, K., Liu, X., Pasternak, F. and Cantié, R.: A geostationary thermal infrared sensor to monitor the lowermost troposphere: O_3 and CO retrieval studies, Atmos. Meas. Tech., 4(2), 297–317, doi:10.5194/amt-4-297-2011, 2011.

Cui, Y. Y., Brioude, J., McKeen, S. a., Angevine, W. M., Kim, S.-W., Frost, G. J., Ahmadov, R., Peischl, J., Bousserez, N., Liu, Z. and Ryerson, T. B.: Top-down estimate of methane emissions in California using a mesoscale inverse modeling technique: The South Coast Air Basin, J. Geophys. Res. Atmos., 120, 6698–6711, doi:10.1002/2014JD023002, 2015.

Edwards, D. P., Arellano, A. F. and Deeter, M. N.: A satellite observation system simulation experiment for carbon monoxide in the lowermost troposphere, J. Geophys. Res., 114(D14), D14304, doi:10.1029/2008JD011375, 2009.

Elbern, H., Strunk, A., Schmidt, H. and Talagrand, O.: Emission rate and chemical state estimation by 4-dimensional variational inversion, Atmos. Chem. Phys., 7(14), 3749–3769, doi:10.5194/acp-7-3749-2007, 2007.

Fishman, J., Iraci, L. T., Al-Saadi, J., Chance, K., Chavez, F., Chin, M., Coble, P., Davis, C., DiGiacomo, P. M., Edwards, D., Eldering, A., Goes, J., Herman, J., Hu, C., Jacob, D. J., Jordan, C., Kawa, S. R., Key, R., Liu, X., Lohrenz, S., Mannino, A., Natraj, V., Neil, D., Neu, J., Newchurch, M., Pickering, K., Salisbury, J., Sosik, H., Subramaniam, A., Tzortziou, M., Wang, J. and Wang, M.: The United States' Next Generation of Atmospheric Composition and Coastal Ecosystem Measurements: NASA's Geostationary Coastal and Air Pollution Events (GEO-CAPE) Mission, Bull. Am. Meteorol. Soc., 93(10), 1547–1566, doi:10.1175/BAMS-D-11-00201.1, 2012.

Gaspari, G., Gaspari, G., Cohn, S. E. and Cohn, S. E.: Construction of correlation functions in two and three dimensions, Q. J. R. Meteorol. Soc., 125(April 1998), 723–757, doi:10.1002/qj.49712555417, 1999.

Gaubert, B., Coman, A., Foret, G., Meleux, F., Ung, A., Rouil, L., Ionescu, A., Candau, Y. and Beekmann, M.: Regional scale ozone data assimilation using an ensemble Kalman filter and the CHIMERE chemical transport model, Geosci. Model Dev., 7(1), 283–302, doi:10.5194/gmd-7-283-2014, 2014.

Guerrette, J. J. and Henze, D. K.: Development and application of the WRFPLUS-Chem online chemistry adjoint and WRFDA-Chem assimilation system, Geosci. Model Dev., 8(6), 1857–1876, doi:10.5194/gmd-8-1857-2015, 2015.

Hache, E., Attié, J.-L., Tourneur, C., Ricaud, P., Coret, L., Lahoz, W. A., El Amraoui, L., Josse, B., Hamer, P., Warner, J., Liu, X., Chance, K., Höpfner, M., Spurr, R., Natraj, V., Kulawik, S., Eldering, A. and Orphal, J.: The added value of a visible channel to a geostationary thermal infrared instrument to monitor ozone for air quality, Atmos. Meas. Tech., 7(7), 2185–2201, doi:10.5194/amt-7-2185-2014, 2014.

5 Hu, X.-M., Nielsen-Gammon, J. W. and Zhang, F.: Evaluation of Three Planetary Boundary Layer Schemes in the WRF Model, J. Appl. Meteorol. Climatol., 49(9), 1831–1844, doi:10.1175/2010JAMC2432.1, 2010.

Kang, J.-S., Kalnay, E., Liu, J., Fung, I., Miyoshi, T. and Ide, K.: "Variable localization" in an ensemble Kalman filter: Application to the carbon cycle data assimilation, J. Geophys. Res., 116(D9), D09110, doi:10.1029/2010JD014673, 2011.

Kang, J.-S., Kalnay, E., Miyoshi, T., Liu, J. and Fung, I.: Estimation of surface carbon fluxes with an advanced data
10 assimilation methodology, J. Geophys. Res. Atmos., 117(D24), n/a–n/a, doi:10.1029/2012JD018259, 2012.

Koohkan, M. R., Bocquet, M., Roustan, Y., Kim, Y. and Seigneur, C.: Estimation of volatile organic compound emissions for Europe using data assimilation, Atmos. Chem. Phys., 13(12), 5887–5905, doi:10.5194/acp-13-5887-2013, 2013.

Kretschmer, R., Gerbig, C., Karstens, U. and Koch, F.-T.: Error characterization of CO_2 vertical mixing in the atmospheric transport model WRF-VPRM, Atmos. Chem. Phys., 12(5), 2441–2458, doi:10.5194/acp-12-2441-2012, 2012.

15 Kretschmer, R., Gerbig, C., Karstens, U., Biavati, G., Vermeulen, a., Vogel, F., Hammer, S. and Totsche, K. U.: Impact of optimized mixing heights on simulated regional atmospheric transport of CO2, Atmos. Chem. Phys., 14(14), 7149–7172, doi:10.5194/acp-14-7149-2014, 2014.

Krotkov, N. a., McLinden, C. a., Li, C., Lamsal, L. N., Celarier, E. a., Marchenko, S. V., Swartz, W. H., Bucsela, E. J., Joiner, J., Duncan, B. N., Boersma, K. F., Veefkind, J. P., Levelt, P. F., Fioletov, V. E., Dickerson, R. R., He, H., Lu, Z. and
20 Streets, D. G.: Aura OMI observations of regional SO<sub>2</sub> and NO<sub>2</sub> pollution changes from 2005 to 2014, Atmos. Chem. Phys. Discuss., 15(19), 26555–26607, doi:10.5194/acpd-15-26555-2015, 2015.

Lahoz, W. A., Peuch, V.-H., Orphal, J., Attié, J.-L., Chance, K., Liu, X., Edwards, D., Elbern, H., Flaud, J.-M., Claeyman, M. and Amraoui, L. El: Monitoring Air Quality from Space: The Case for the Geostationary Platform, Bull. Am. Meteorol. Soc., 93(2), 221–233, doi:10.1175/BAMS-D-11-00045.1, 2012.

25 Laughner, J. L., Zare, A. and Cohen, R. C.: Effects of daily meteorology on the interpretation of space-based remote sensing of NO2, Atmos. Chem. Phys. Discuss., (July), 1–27, doi:10.5194/acp-2016-536, 2016.

Lauvaux, T. and Davis, K. J.: Planetary boundary layer errors in mesoscale inversions of column-integrated CO 2 measurements, J. Geophys. Res. Atmos., 119(2), 490–508, doi:10.1002/2013JD020175, 2014.

Liu, J., Fung, I., Kalnay, E. and Kang, J.-S.: CO 2 transport uncertainties from the uncertainties in meteorological fields,
30 Geophys. Res. Lett., 38(12), n/a–n/a, doi:10.1029/2011GL047213, 2011.

Miyazaki, K., Eskes, H. J., Sudo, K., Takigawa, M., van Weele, M. and Boersma, K. F.: Simultaneous assimilation of satellite NO2, O3, CO, and HNO3 data for the analysis of tropospheric chemical composition and emissions, Atmos. Chem. Phys. Discuss., 12(7), 16131–16218, doi:10.5194/acpd-12-16131-2012, 2012.

Miyazaki, K., Eskes, H., Sudo, K., Boersma, K. F., Bowman, K. and Kanaya, Y.: Decadal changes in global surface NO_x emissions from multi-constituent satellite data assimilation, Atmos. Chem. Phys. Discuss., 0(2), 1–48, doi:10.5194/acp-2016-529, 2016.

Mizzi, A. P., Arellano Jr., A. F., Edwards, D. P., Anderson, J. L. and Pfister, G. G.: Assimilating compact phase space
5   retrievals of atmospheric composition with WRF-Chem/DART: a regional chemical transport/ensemble Kalman filter data assimilation system, Geosci. Model Dev., 9(3), 965–978, doi:10.5194/gmd-9-965-2016, 2016.

Pagowski, M. and Grell, G. A.: Experiments with the assimilation of fine aerosols using an ensemble Kalman filter, J. Geophys. Res. Atmos., 117(D21), n/a–n/a, doi:10.1029/2012JD018333, 2012.

Romine, G. S., Schwartz, C. S., Snyder, C., Anderson, J. L. and Weisman, M. L.: Model Bias in a Continuously Cycled
10   Assimilation System and Its Influence on Convection-Permitting Forecasts, Mon. Weather Rev., 141(4), 1263–1284, doi:10.1175/MWR-D-12-00112.1, 2013.

Russell, A. R., Perring, A. E., Valin, L. C., Bucsela, E. J., Browne, E. C., Wooldridge, P. J. and Cohen, R. C.: A high spatial resolution retrieval of NO_2 column densities from OMI: method and evaluation, Atmos. Chem. Phys., 11(16), 8543–8554, doi:10.5194/acp-11-8543-2011, 2011.

15   Russell, A. R., Valin, L. C. and Cohen, R. C.: Trends in OMI NO_2 observations over the United States: effects of emission control technology and the economic recession, Atmos. Chem. Phys., 12(24), 12197–12209, doi:10.5194/acp-12-12197-2012, 2012.

Saide, P. E., Kim, J., Song, C. H., Choi, M., Cheng, Y. and Carmichael, G. R.: Assimilation of next generation geostationary aerosol optical depth retrievals to improve air quality simulations, Geophys. Res. Lett., 9188–9196,
20   doi:10.1002/2014GL062089.Received, 2014.

Stockwell, W. R., Middleton, P., Chang, J. S. and Tang, X.: The second generation regional acid deposition model chemical mechanism for regional air quality modeling, J. Geophys. Res., 95(D10), 16343, doi:10.1029/JD095iD10p16343, 1990.

Travis, K. R., Jacob, D. J., Fisher, J. a., Kim, P. S., Marais, E. a., Zhu, L., Yu, K., Miller, C. C., Yantosca, R. M., Sulprizio, M. P., Thompson, A. M., Wennberg, P. O., Crounse, J. D., St. Clair, J. M., Cohen, R. C., Laugher, J. L., Dibb, J. E., Hall, S.
25   R., Ullmann, K., Wolfe, G. M., Pollack, I. B., Peischl, J., Neuman, J. a. and Zhou, X.: NO_x emissions, isoprene oxidation pathways, vertical mixing, and implications for surface ozone in the Southeast United States, Atmos. Chem. Phys. Discuss., (2), 1–32, doi:10.5194/acp-2016-110, 2016.

Turner, A. J., Jacob, D. J., Wecht, K. J., Maasakkers, J. D., Lundgren, E., Andrews, A. E., Biraud, S. C., Boesch, H., Bowman, K. W., Deutscher, N. M., Dubey, M. K., Griffith, D. W. T., Hase, F., Kuze, A., Notholt, J., Ohyama, H., Parker, R.,
30   Payne, V. H., Sussmann, R., Sweeney, C., Velazco, V. A., Warneke, T., Wennberg, P. O. and Wunch, D.: Estimating global and North American methane emissions with high spatial resolution using GOSAT satellite data, Atmos. Chem. Phys., 15(12), 7049–7069, doi:10.5194/acp-15-7049-2015, 2015.

Valin, L. C., Russell, A. R., Hudman, R. C. and Cohen, R. C.: Effects of model resolution on the interpretation of satellite NO_2 observations, Atmos. Chem. Phys., 11(22), 11647–11655, doi:10.5194/acp-11-11647-2011, 2011.

35   Valin, L. C., Russell, A. R. and Cohen, R. C.: Variations of OH radical in an urban plume inferred from NO_2 column measurements, Geophys. Res. Lett., 40(9), 1856–1860, doi:10.1002/grl.50267, 2013.

Yumimoto, K.: Impacts of geostationary satellite measurements on CO forecasting: An observing system simulation experiment with GEOS-Chem/LETKF data assimilation system, Atmos. Environ., 74, 123–133, doi:10.1016/j.atmosenv.2013.03.032, 2013.

5   Zoogman, P., Jacob, D. J., Chance, K., Worden, H. M., Edwards, D. P. and Zhang, L.: Improved monitoring of surface ozone by joint assimilation of geostationary satellite observations of ozone and CO, Atmos. Environ., 84, 254–261, doi:10.1016/j.atmosenv.2013.11.048, 2014.

Zoogman, P., Liu, X., Suleiman, R. M., Pennington, W. F., Flittner, D. E., Al-Saadi, J. a., Hilton, B. B., Nicks, D. K., Newchurch, M. J., Carr, J. L., Janz, S. J., Andraschko, M. R., Arola, a., Baker, B. D., Canova, B. P., Chan Miller, C., Cohen, R. C., Davis, J. E., Dussault, M. E., Edwards, D. P., Fishman, J., Ghulam, a., Gonz??lez Abad, G., Grutter, M., Herman, J. R.,
10   Houck, J., Jacob, D. J., Joiner, J., Kerridge, B. J., Kim, J., Krotkov, N. a., Lamsal, L., Li, C., Lindfors, a., Martin, R. V., McElroy, C. T., McLinden, C., Natraj, V., Neil, D. O., Nowlan, C. R., O??Sullivan, E. J., Palmer, P. I., Pierce, R. B., Pippin, M. R., Saiz-Lopez, a., Spurr, R. J. D., Szykman, J. J., Torres, O., Veefkind, J. P., Veihelmann, B., Wang, H., Wang, J. and Chance, K.: Tropospheric emissions: Monitoring of pollution (TEMPO), J. Quant. Spectrosc. Radiat. Transf., 186(2017), 17–39, doi:10.1016/j.jqsrt.2016.05.008, 2017.

15

Table 1. The experimental set up of each assimilation run. The three ensemble runs assimilate NO_2 observations every hour, and differ in treatment of meteorology forecast.

Experiment	Met Assim	Chem Assim	note
REF	No	Yes	Truth meteorology
ENS.1	Yes	Yes	Ensemble of meteorology and chemistry
ENS.2	Yes	Yes	Only update emissions
ENS.3	Yes	Yes	Initial meteorology ensemble is from the next day
REA	No	Yes	Using ensemble mean from ENS.1

5

Table 2. DART configurations.

Parameter	Value
Filter type	EAKF
Adaptive inflation	1.0, 0.6 (initial mean, spread)
Inflation damping	0.9
Adaptive localization threshold	2000
Localization type	Gaspari-Cohn
Horizontal localization half-width for meteorology (chemical) observation	50 km (10 km)
Outlier threshold	3.0
Ensemble members	30

10

19

Table 3. WRFDA configurations.

Parameter	Value
cv_options	3 (NCEP background error model)
je_factor (ensemble covariance weighting factor)	1.0

5

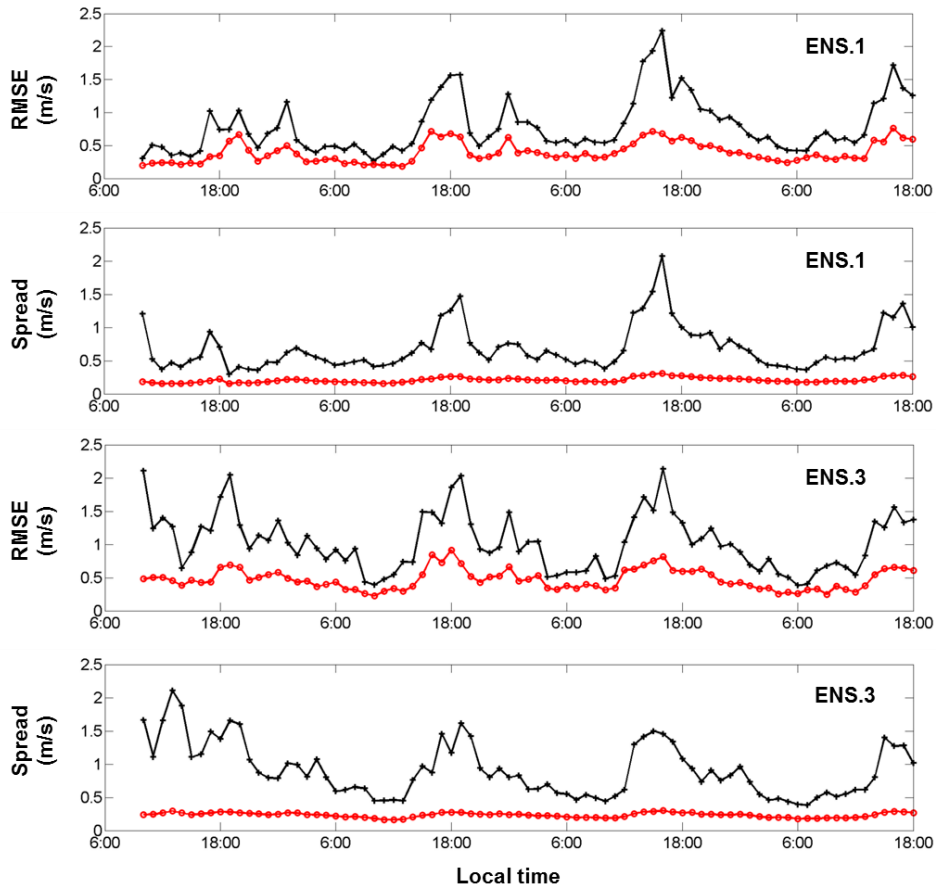**Table 4.** <mark>Relative observation uncertainty σ_{rel} in synthetic TEMPO NO$_2$ column for each scenario.</mark>

Type	NO$_2$ column	Gaussian distribution
Clean	$<0.3\times10^{15}$ molec. com^{-2}	N (200%, 100%)
Polluted	$>=0.3\times10^{15}$ molec. com^{-2}	N (7.5%, 2.5%)
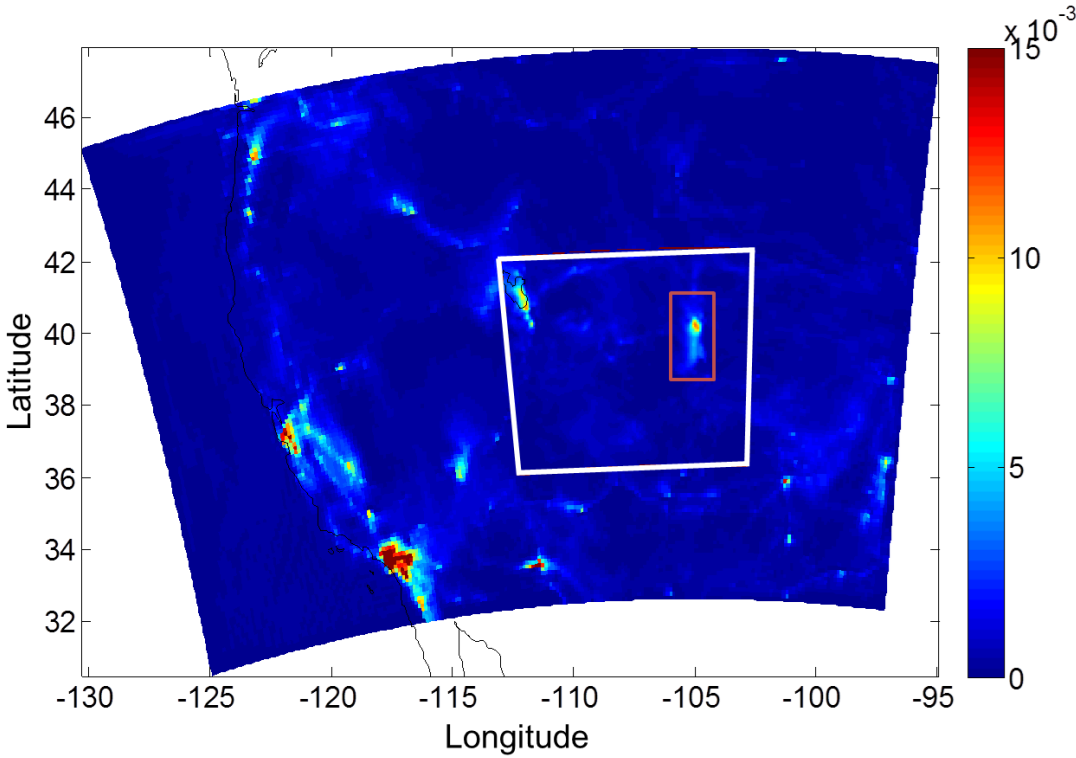
10

5
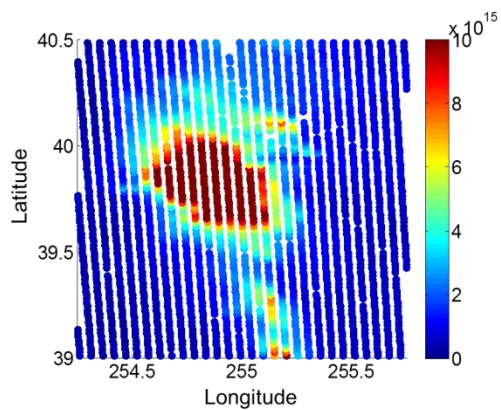
**Figure 2.** Example of synthetic TEMPO NO$_2$ column observations over Denver, CO at 17:00 LT July 2nd in 2014.

Figure 3. Time evolution of prior (black) and posterior (red) RMSE and spread of surface mesonet zonal wind observation in Denver from July 2nd 10:00 to 5th 18:00 for ENS.1 (top) and ENS.3 (bottom).

5
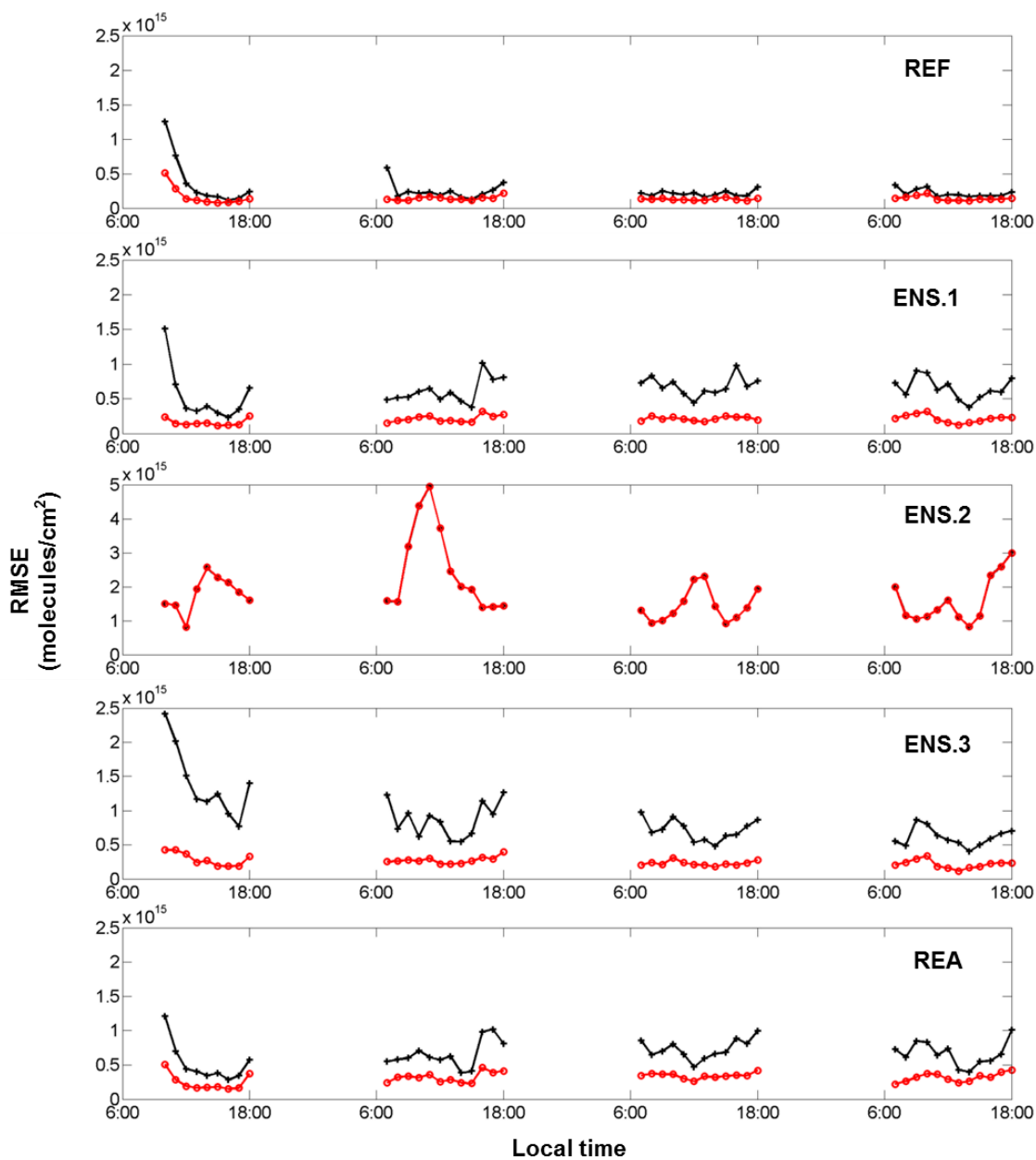
Figure 4. Time evolution of prior (black) and posterior (red) RMSE of Denver TEMPO NO$_2$ column observation from July 2nd 10:00 to 5th 18:00 for REF, ENS.1, ENS.2, ENS.3 and REA (from top to bottom).

5
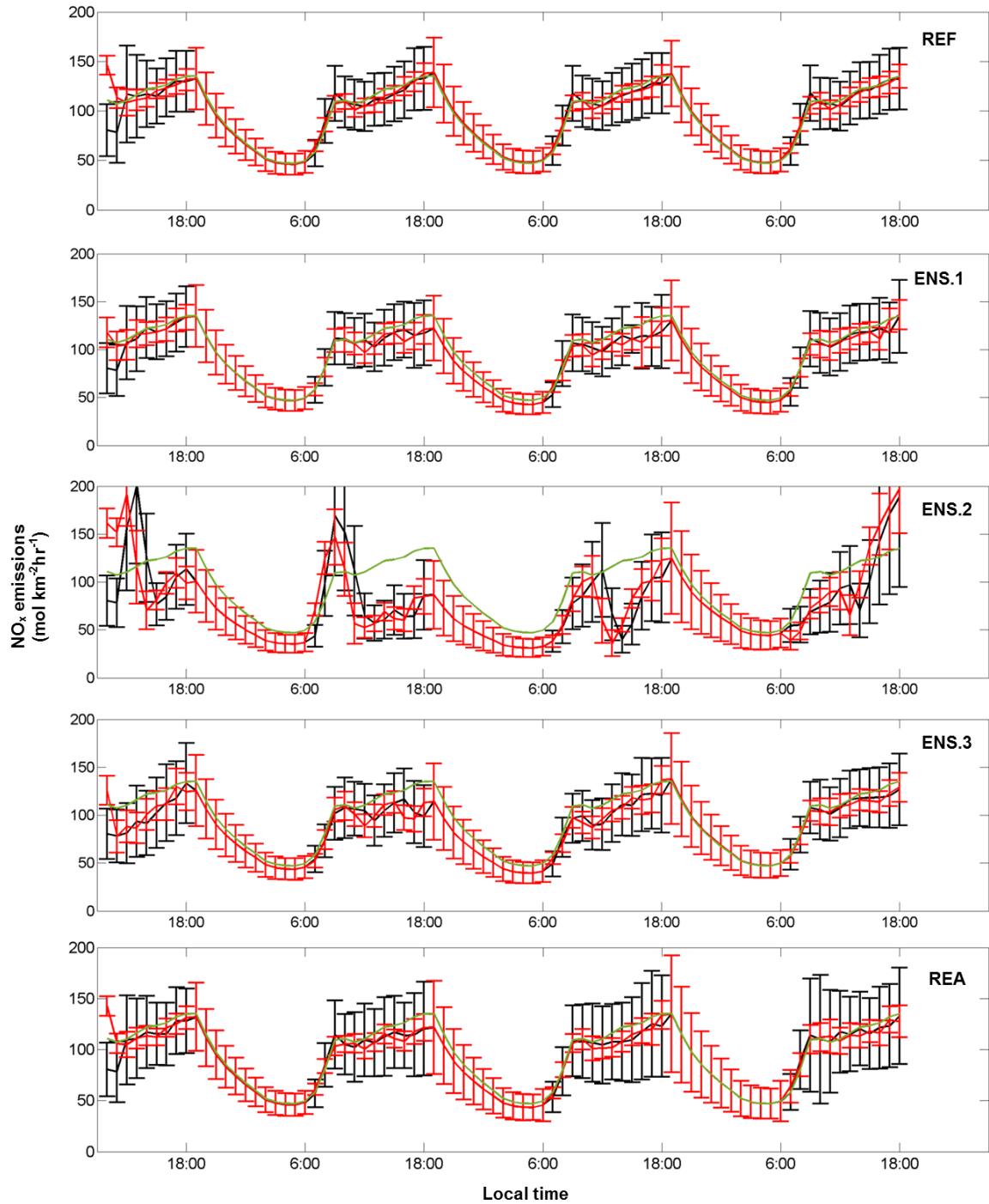
Figure 5. Time evolution of averaged Denver city emission of prior (black), posterior (red) and truth (green) for REF, ENS.1, ENS.2, ENS.3 and REA (from top to bottom).The error bar is defined by the ensemble spread and represents the uncertainty of the prior and posterior estimates.
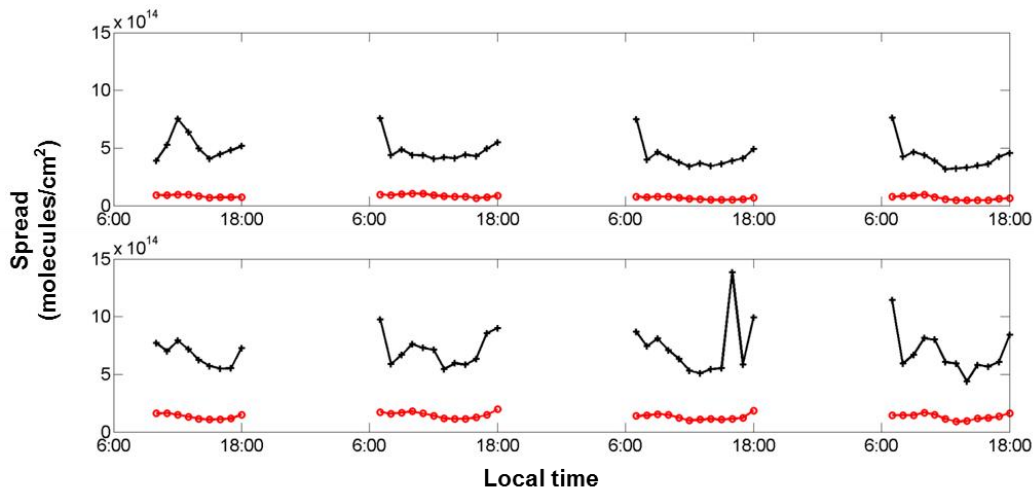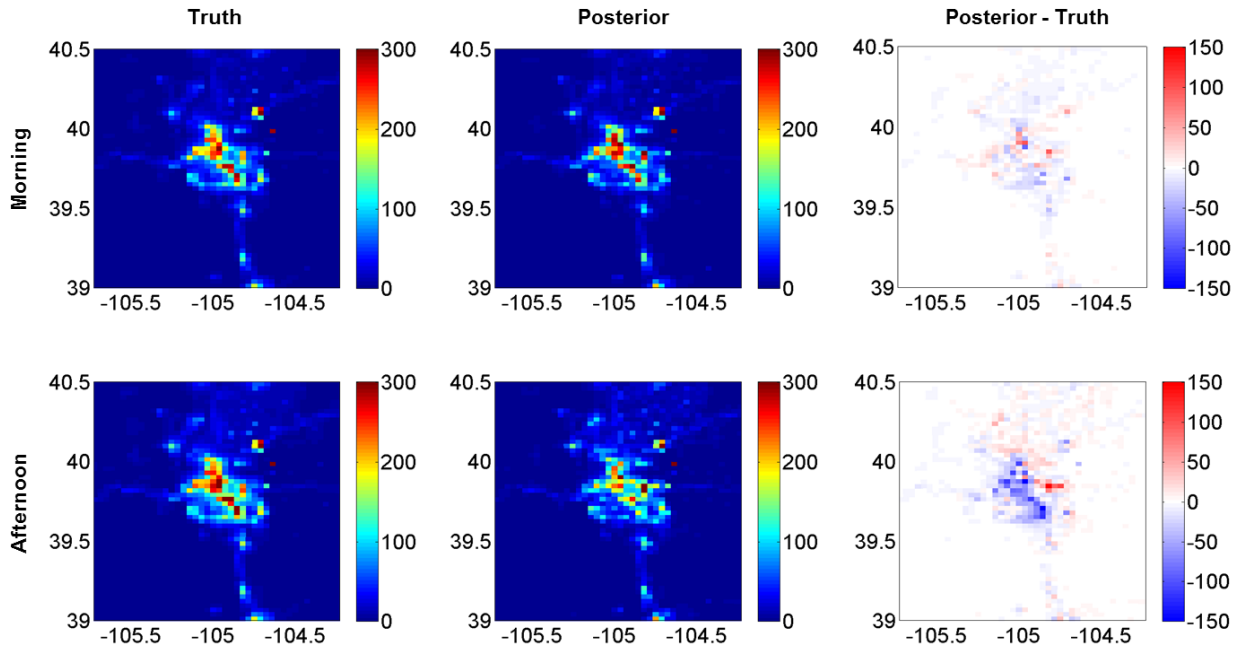
Figure 6. Time evolution of prior (black) and posterior (red) spread of Denver TEMPO NO_2 column observation from July 2nd 10:00 to 5th 18:00 for REF (top) and ENS.1 (bottom).

5
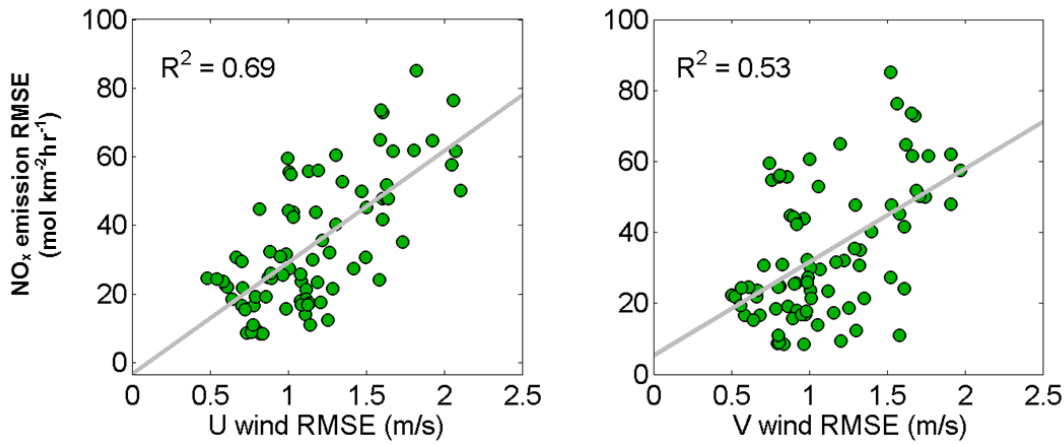
Figure 7. The scatter plot between the prior RMSE of boundary layer wind vectors and urban NO_x emission posterior RMSE over four-day daytime assimilation time period in ENS.1.

10

25

Figure 8. The emission estimation results in ENS.1 at 9:00 am (top) 4:00 pm (bottom) on July 3rd of truth, posterior and the difference between truth and posterior (from left to right). The unit is mol km^{-2}hr^{-1}.